Dynamical properties of the TRIFFID dynamic global vegetation model

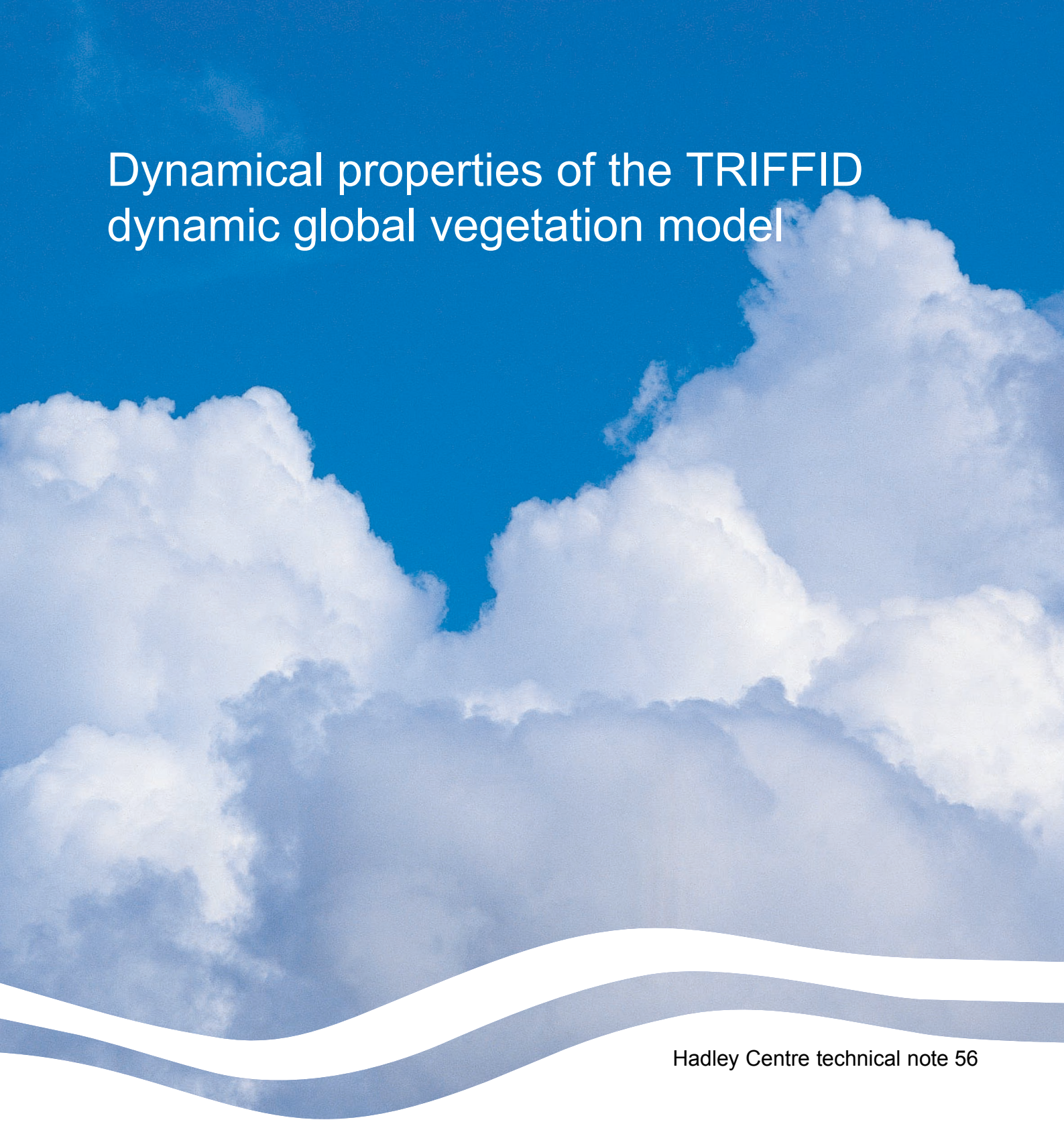

Hadley Centre technical note 56

J.K.Hughes, P.J.Valdes, R.A.Betts

8 October 2004

Met Office

Dynamical properties of the TRIFFID dynamic global vegetation model.

J.K.Hughes[1], P.J. Valdes[1], R.A.Betts[2]
[1] Geographical Sciences, University of Bristol, University Road, BS8 1SS, UK
[2] Met Office, Hadley Centre, FitzRoy Road, Exeter, Devon, EX1 3PB, UK.
J.K.Hughes@bristol.ac.uk

October 12, 2004

Abstract

This note describes the dynamical properties of the terrestrial vegetation structure represented in the Hadley Centres coupled climate-carbon cycle model. Investigating the dynamical properties of the terrestrial vegetation structure provides an understanding of the causes of variability of the land surface properties, which are important in land-atmosphere interactions. In order to investigate the vegetation structure mathematically a simplified version of the TRIFFID vegetation model is derived. TRIFFID is shown to be dynamically stable, and converges towards an equilibrium balance of carbon fluxes; *i.e.* TRIFFID is not intrinsically sensitive to the choice of initial vegetation structure, though the behaviour of the full climate model may be. Analysis of the underlying equations demonstrates that competing TRIFFID vegetation types can coexist in a single grid box, and that there is potentially a smooth transition between regions dominated by one competing vegetation type to another. The stability of TRIFFID means that variability of land surface properties is therefore driven by variability of atmospheric conditions. TRIFFID does however attenuate atmospheric variability, and is a source of red noise. The timescale for a recovery of vegetation structure from perturbations and the maximum rate of growth are investigated and are shown to relate to the predicted net primary productivity. The time taken for trees to recover from a extreme perturbation is shown to be of the order of 125 years. This timescale is validated against recovery of forest cover after the 1908 Tunguska meteorite impact. Investigation of the Tunguska recovery also demonstrates a scale dependence of the spectral response of TRIFFID to perturbations. The recovery timescale also governs the spectral attenuation. This means that the spectral properties of TRIFFID are sensitive to changes in atmospheric carbon dioxide levels and climatic conditions.

1 Introduction

Advances in the representation of the land surface in general circulation models (GCMs) has been made over the past decades, and the most advanced GCMs now incorporate representations of the land surface which are not static, but can change in response to changes in the atmospheric state. For example in these models the distributions of desert regions can vary. In developing dynamic global vegetation models (DGVMs)

choices must be made concerning the underlying behavioural properties that global vegetation is assumed to exhibit.

The Hadley Centre's TRIFFID model couples a photosynthesis model (Cox *et al.* (1998)) to a population model (in the ecological sense). The population model updates the fractional coverage and height of vegetation depending on the predicted photosynthesis. This population model therefore plays a large role in the dynamic properties of the land surface. The TRIFFID model is described by Cox (2001). Cox (2001) discuss the photosynthesis model and the way that environmental conditions are translated into predicted net primary productivity (NPP) rates. This report will investigate the population model, and derive a simple version of the population model used in TRIFFID which helps give greater insight into the fundamental processes and interactions.

In section 2 standard analysis of the type of population model (Lotka-Volterra competition equations) is reproduced. This is then linked to the TRIFFID model parameters. The diffusive Lotka-Volterra competition equations are also investigated, and these results are then linked to the TRIFFID model. Analysis of the Lotka-Volterra competition equations is not new, but it is necessary to reproduce it here, to be able to investigate the TRIFFID equations. Few ecological textbooks contain the analysis of the diffusive equations, but it is a very simple addition to the investigation of the non-diffusive equations. In section 3 the assumption of a single dominant plant functional type at a particular grid box is tested. Using simulated plant functional type distributions from a pre-agricultural control simulation the mutually exclusive nature of competing plant functional types is demonstrated. In section 4 the simplified form of TRIFFID is derived. In section 5 the ability of the simplified form of TRIFFID to predict the vegetation dynamics is verified, and in section 6 the steady state solution of the simplified TRIFFID model is discussed. In the next section the initial growth rate of the simplified TRIFFID model is analysed. In section 8 the maximum rate of expansion of fractional coverage is derived, and the stability of the model is discussed. Internal variability and the interaction with stochastic forcing is analysed in section 9. In section 10 the re-growth timescale of needleleaf tree PFT is compared with the recovery of real forest to a grid box scale cosmic perturbation. The extent that the simplified model captures the behaviour of the full TRIFFID model and the lessons learnt from this study will be discussed in section 11.

Using a similar approach to that presented here, Huntingford *et al.* (2000) present a simplified version of the terrestrial carbon cycle. Huntingford *et al.* (2000) also reduce the vegetation dynamics to a single plant functional type (assumed to be a tree PFT). The model of Huntingford *et al.* (2000) incorporates a representation of soil carbon dynamics and photosynthesis. As a result of this approach, Huntingford *et al.* (2000) focus on simulating the response to increasing CO_2 levels. Whilst the study of Huntingford *et al.* (2000) focussed on the impact of environmental change, the simplified model presented here will be used to investigate the dynamical properties of the vegetation model, interpreting the results of this to help understand how the vegetation model behaves in the full GCM system. Several of the assumptions made by Huntingford *et al.* (2000) and also in this report are evaluated here. The links between the simplified model presented here and the full complexity TRIFFID model are made explicit, and the ability of the simplified model to capture the behaviour of TRIFFID is tested; this was not performed by Huntingford *et al.* (2000). In future studies the TRIFFID model will be investigated within a full GCM system, allowing vegetation to dynamically interact with the atmosphere. The analysis presented in this report will help interpretation of these simulations.

In order to test the simplified model aginst full complexity TRIFFID model a pre-agriculture simulation was completed using the Hadley Centre's climate model, HadSM3. HadSM3 uses a thermodynamic 'slab' representation of the ocean. Modern heat convergences are used here. The atmosphere is represented with 3.75 degrees by 2.50 degrees resolution, and 19 vertical levels. Atmospheric CO_2 is held constant at 287 ppmv. Agricultural disturbances are set to zero coverage.

2 Competition solution

In this section the now classic analysis of Lotka-Volterra competition equations is reproduced (see Case (2000) pp. 316-327). This analysis is then related to the specific case of the TRIFFID model. The Lotka-Volterra analysis is then extended to consider diffusive Lotka-Volterra competition equations. One modification to the Lotka-Volterra equations is to introduce the effects of harvesting. This is a steady reduction in population and is usually either a constant rate or proportional to the population size. If the decrease in population size is greater than a population's ability to increase, then the population size will decrease towards extinction. For this reason Lotka-Volterra competition equations including the effects of grazing or harvesting are said to be diffusive (Case (2000), p. 137). The TRIFFID model is based on diffusive Lotka-Volterra competition equations.

The original Lotka-Volterra competition equations for two species are given by eqns. 1 and 2 (*e.g.* Gotelli (1998),p. 101).

$$\frac{dN_1}{dt}\frac{1}{N_1} = \frac{r_1}{K_1}(K_1 - N_1 - c_1 N_2) \quad (1)$$

$$\frac{dN_2}{dt}\frac{1}{N_2} = \frac{r_2}{K_2}(K_2 - N_2 - c_2 N_1) \quad (2)$$

N_1 and N_2 are population sizes for two competing species (*e.g.* between grasses). Coefficients c_1 and c_2 are the competition coefficients, and quantify the ability of one species to restrict the expansion of another species. r_1 and r_2 are the intrinsic growth rates for N_1 and N_2 respectively. K_1 and K_2 are the maximum magnitudes of N_1 and N_2 that can be supported by their environment.

In TRIFFID, shrub dominates grasses (i.e. it always displaces grass fractional coverage). Trees dominate both grasses and shrub. However between plant functional types on the same level of this dominance hierarchy competition is resolved with Lotka-Volterra competition for space. To derive the possible solutions of the Lotka-Volterra competition equations we consider the necessary conditions under which a population will persist under the least favourable conditions possible in the Lotka-Volterra equations. For species N_1 this is when $N_2 \sim K_2$, and N_1 is close to 0, *i.e.* the conditions $(\mathrm{d}N_1/\mathrm{dt})(1/N_1) > 0$, when N_1 tends to zero, and N_2 tends to K_2. Then we have

$$\frac{dN_1}{dt}\frac{1}{N_1} \approx \frac{r_1}{K_1}(K_1 - 0 - c_1 K_2) \quad (3)$$

For $\frac{dN_1}{dt}\frac{1}{N_1} > 0$, since $r_1 > 0$ by definition, we get eqn. 4.

$$\frac{K_1}{K_2} > c_1 \tag{4}$$

By considering what conditions are required for N_2 to expand, when $N_1 = K_1$ and N_2 is close to 0 we get inequality (5).

$$\frac{K_2}{K_1} > c_2 \tag{5}$$

Now each inequality (eqns. 4 and 5) is either satisfied, or not, generating 4 possible combinations.

Case 1: N_2 does not satisfy eqn. 5, and will not persist, but N_1 satisfies eqn. 4 and persists. This leads to the case where N_1 out-competes N_2 with the steady state solution $N_1 = K_1$, $N_2 = 0$, fig. 1(a).

Case 2: The reverse of Case 1 , N_2 satisfies eqn. 5, but N_1 doesn't satisfy equality 4, leading to the solution N_1=0, N_2=K_2, fig. 1(b)

Case 3: Both N_1 and N_2 persist as equality 4 and 5 are both satisfied, and a stable co-existence is reached, fig. 1(c).

Case 4: Neither eqn. 4 5 are satisfied, and N_1 and N_2 are in unstable equilibrium, fig. 1(d).

Exact solutions of the Lotka-Volterra competition equations are found when the time derivatives of the Lotka-Volterra competition equations are set to zero. This leads to eqns. 6 and 7

$$N_1 = K_1 - c_1 N_2 \tag{6}$$
$$N_2 = K_2 - c_2 N_1 \tag{7}$$

Then the four different cases simply refer to the 4 different ways of plotting the two solution lines.

In fig. 1 the arrow triplets show the direction both the populations move in, for a specific region of the graph. To the right of the steady state line for N_1, $N_1 > K_1$, i.e. the population of N_1 is too large to be supported, and N_1 decreases (moves to the left). Therefore the plots allow the behaviour to be predicted for any point on the N_1,N_2 plane.

The TRIFFID model is constrained to case 3 by the following assumptions (which are built into TRIFFID): c_1 and c_2 are always less than 1.0, and $K_1 = K_2$. As $\frac{K_1}{K_2} = 1$, and c_1 is < 1 eqn. 4 is satisfied. $\frac{K_2}{K_1} = 1$ and $c_2 < 1$, satisfying eqn. 5, so we have the

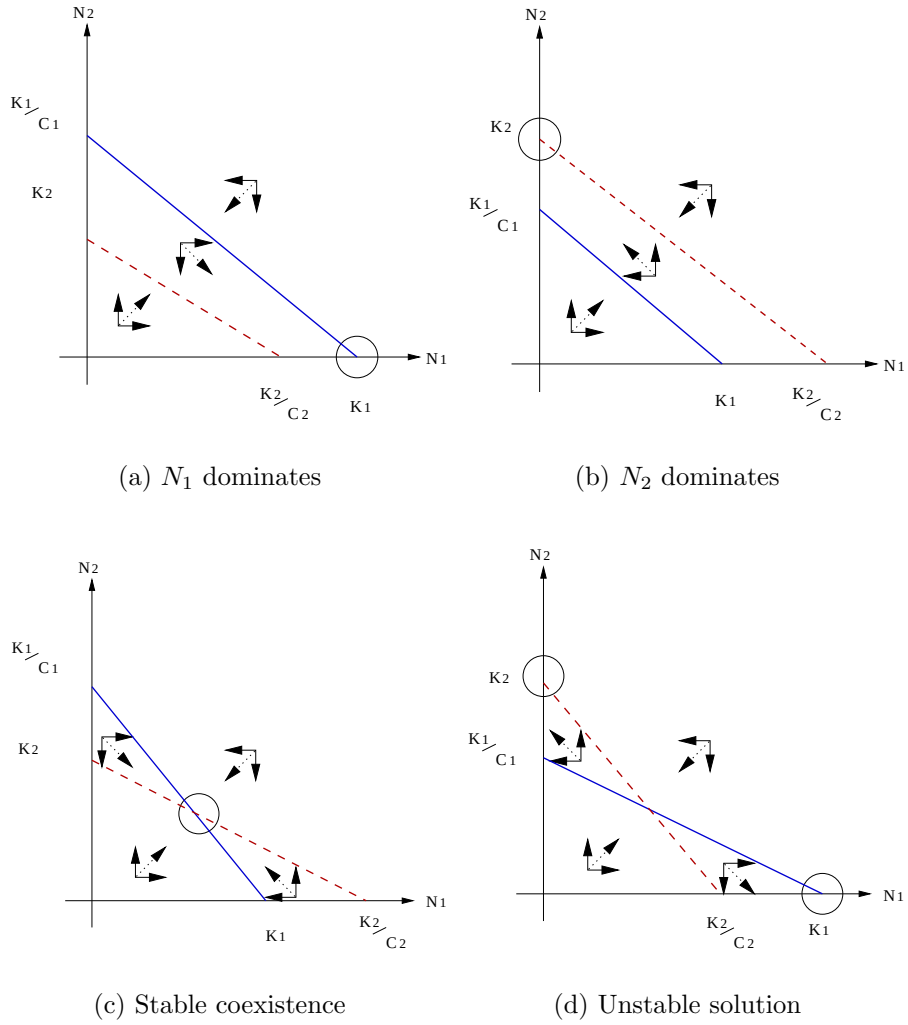

(a) N_1 dominates (b) N_2 dominates

(c) Stable coexistence (d) Unstable solution

Figure 1: *The four possible solutions of the Lotka-Volterra model. The lines correspond to the equilibrium solutions of the Lotka-Volterra model. The solid, blue line is the equilibrium solution for species N_1. The dashed, red line is the equilibrium solution for species N_2. The circles indicate the final solution in each case. Reproduced from Gotelli (1998), pp. 107-114. The x-axis shows the magnitude of population N_1. The y-axis shows the magnitude of population N_2. The arrow triplets indicate the direction of change of both populations, in a particular region of the graph. The dotted arrow in the triplet indicates the net movement on the graph.*

case of stable co-existence. In the TRIFFID model setup non-diffusive Lotka-Volterra competition equations must be constrained to case 3 because the total fractional coverages must sum to 100 %, and dominant PFTs impose the same reduction in space for both of the two competing species. If, however, competition were for something other than fractional coverage these assumptions might not necessarily apply, and other cases would be possible.

The above analysis ignored diffusion. TRIFFID uses a diffusive version of the Lotka-Volterra competition equations, which become:

$$\frac{dN_1}{dt}\frac{1}{N_1} = \frac{r_1}{K_1}(K_1 - N_1 - c_1 N_1) - \gamma_1 \quad (8)$$

$$\frac{dN_2}{dt}\frac{1}{N_2} = \frac{r_2}{K_2}(K_2 - N_2 - c_2 N_2) - \gamma_2 \quad (9)$$

and the inequalities 4 and 5 become :

$$\frac{K_1}{K_2} > c_1 + \frac{\gamma_1}{r_1}\frac{K_1}{K_2} \quad (10)$$

$$\frac{K_2}{K_1} > c_2 + \frac{\gamma_2}{r_2}\frac{K_2}{K_1} \quad (11)$$

γ is the natural disturbance rate, including such effects as fire and herbivory. Constraining these inequalities to the properties of TRIFFID, using the same assumptions as the non-diffusive case, the inequalities become:

$$1 - \frac{\gamma_1}{r_1} > c_1 \quad (12)$$

$$1 - \frac{\gamma_2}{r_2} > c_2 \quad (13)$$

The equilibrium solutions of the diffusive Lotka-Volterra equations are :

$$N_1 = K_1(1 - \frac{\gamma_1}{r_1}) - c_1 N_2 \quad (14)$$

$$N_2 = K_2(1 - \frac{\gamma_2}{r_2}) - c_2 N_1 \quad (15)$$

The effect of diffusion is to force a translation of the solution lines, parallel to the axis. It has now been shown that for the non diffusive case, constraining the Lotka-Volterra competition equations to the TRIFFID choice of parameters forces stable coexistence of the two species. As can be seen from eqns. 12 and 13, when $r_1 >> \gamma_1$ and $r_1 >> \gamma_2$ the diffusive TRIFFID model is constrained to the case of stable coexistence. When these inequalities are not satisfied the other three cases are also possible.

When the two equalities are met, and there is stable coexistence, N_1 and N_2 are given by eqns. 16 and 17

$$N_1 = [K_1(1 - \frac{\gamma_1}{r_1}) - c_1 K_2(1 - \frac{\gamma_2}{r_2})](1 - c_1 c_2)^{-1} \quad (16)$$

$$N_2 = [K_2(1 - \frac{\gamma_2}{r_2}) - c_2 K_1(1 - \frac{\gamma_1}{r_1})](1 - c_1 c_2)^{-1} \quad (17)$$

When eqns. 12 and 13 are not both met then either $N_1 = K_1(1 - \frac{\gamma_1}{r_1})$ or $N_2 = K_2(1 - \frac{\gamma_2}{r_2})$, depending on which of the inequalities is satisfied, and the other fractional coverage is at most that which can exist in the space left by the dominant species, N_2 = 1 - K_1(1-$\frac{\gamma_1}{r_1}$), or N_1 = 1 - K_2(1-$\frac{\gamma_2}{r_2}$).

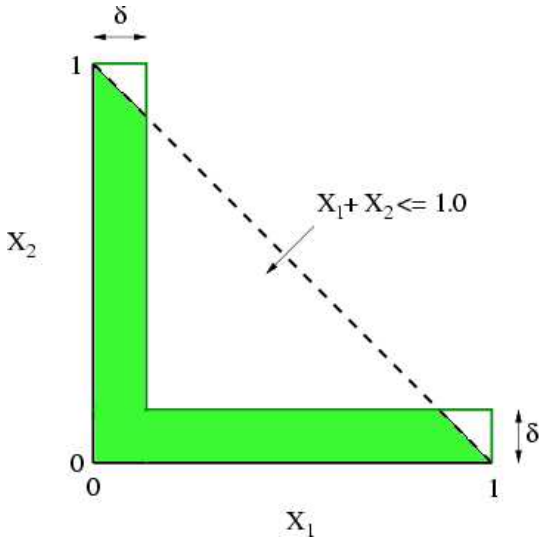

Figure 2: *Delta function. X_i is the fractional coverage of species i. The Triangular region, bounded by the points [(0,0), (0,1), (1,0)] is the range of possible combinations of X_1, and X_2. The ratio of the number of points within the green shaded region to the total number of points is calculated. When δ is small only points that are approximately equal to [X_1,0] or [0, X_2] are in the green region.*

3 The single species assumption

In the rest of this report we investigate the properties of a single species version of TRIFFID. This is equivalent to assuming that grid boxes are dominated by only one PFT of a competing pair of PFTs (*e.g.* broadleaf and needleleaf trees.). The previous section showed that the Lotka-Volterra competition equations do not exclude the possibility of coexistence, but the physical parameters of the different PFTs suggest that they may thrive in different environments (see Cox (2001)). In order to justify the assumption of a single, dominant fractional coverage of vegetation, the simulated pre-agricultural vegetation is analysed. If vegetation is mutually exclusive, then in a scatter plot of the two fractional coverages, the points will lie on the axis. The further from the axis the points are, the less reliable is the assumption of a single dominant species.

In order to quantify the validity of the single species assumption the number of points found within a region, δ, of the axes is calculated and expressed as the ratio to the total number of points. This ratio is calculated for δ ranging between zero and 0.5 (when it includes all the possible values), and is illustrated in fig. 2. It can be shown that if the points are uniformly distributed then the ratio of points within the δ region (equivalent to the area of the region) to the total number of points (or area) is equal to $1-(1-2\delta)^2$, neglecting the effects of diffusion, which varies from grid box to grid box.

Discounting zero coverage grid boxes produces four datasets of pre-agricultural fractional coverages, of 2,381 points. These datasets actually incorporate a total of 2,571,480 data points as the pre-agricultural vegetation is a mean of 30 years of data, at 10 day resolution. Plots of the ratio of points within the δ region to the total number of plots are shown for the grasses and the trees in fig. 3. Figure 3 also plots the uniform distribution assumption, $1-(1-2\delta)^2$, for comparison.

Figure 3 shows that the distribution of points is significantly clustered around the

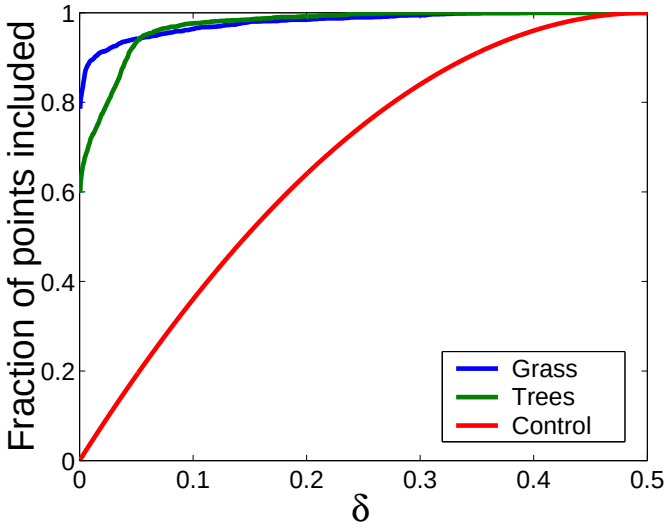

Figure 3: *The δ test for simulated coexistence, for the grass PFTs (blue line), and the tree PFTs (green line). Also shown is is the control ratio (red line), i.e. how the fraction would increase as a function of δ if the fractional coverages were uniformly distributed.*

axis, i.e. for the simulation of steady state, pre-agriculture vegetation, vegetation is largely either C3 or C4 type grass, or either broadleaf or needleleaf tree, at a particular grid box. Figure 3 suggests that the assumption of a single dominant plant functional type is reasonable. For pre-agricultural grasses, 96 % of grass is found within the $\delta = 0.05$ region. For tree plant functional types, 94% is found within the $\delta = 0.05$ region. Figure 3 shows that if the plant functional types were uniformly distributed this percentage would be close to 20 %.

4 Derivation of simplified TRIFFID

Having justified the assumption of single PFT, in this section the simplified TRIFFID model is derived. The litterfall rate, Λ_l, and the disturbance parameter, γ_ν are assumed to be a constant. By reducing the TRIFFID model to a single PFT, we restrict the use of the simplified model to predicting the behaviour of the dominant PFT.

The main dynamic vegetation equations in the TRIFFID model represent the relationship between vegetation carbon density and fractional coverage (see Cox (2001)). The equations are:

$$\frac{dC_\nu}{dt} = (1-\lambda)\Pi - \Lambda_l \tag{18}$$

$$C_\nu \frac{d\nu}{dt} = \lambda\Pi\nu_*(1 - \sum_j c_{ij}\nu_j) - \gamma_\nu \nu_* C_\nu \tag{19}$$

C_ν is the vegetation carbon density of the PFT, Π is the NPP, Λ_l is the litterfall rate on PFT, and represents the loss of carbon matter resulting from the natural life cycle of the vegetation. ν_i is the fractional coverage of PFT i. ν_* is the fractional coverage of PFT i, if ν_i greater than 0.001 %, otherwise $\nu_* = 0.001$ %. γ_ν is a disturbance parameter and implicitly incorporates the effects of mortality arising from processes other

than competition with other PFTs, *e.g.* fire, disease, and herbivory into TRIFFID. λ is defined in expression 20. λ controls the partitioning of NPP between fractional coverage expansion and increasing the carbon density.

$$\lambda = \begin{cases} 1 & \text{for } L_b > L_{max} \\ \frac{L_b - L_{min}}{L_{max} - L_{min}} & \text{for } L_{min} < L \leq L_{max} \\ 0 & \text{for L} \leq L_{min} \end{cases} \tag{20}$$

L is the Leaf area index (LAI), and L_{min} and L_{max} are minimum and maximum LAI values, and are specified for each PFT. c_{ij} is the intra-species competition term between species i and species j, as described by table 1, and eqn. 21.

	i=1	i=2	i=3	i=4	i=5
j=1		*	1	1	1
j=2	*		1	1	1
j=3	0	0		1	1
j=4	0	0	0		*
j=5	0	0	0	*	

Table 1: *Intra- species competition relationships. Numbers $i = 1, 5$ represents plant functional types: broadleaf tree, needleleaf tree, shrub, C3 type grass, and C4 type grass. Entry '*' is given by eqn. 21. A value of 0 implies that PFT i dominates PFT j. A value of* 1 *implies PFT j dominates PFT i.*

$$c_{ij} = \frac{1}{1 + exp\{20(height_i - height_j)/(height_i + height_j)\}} \tag{21}$$

$height_i$ is the vegetation height of PFT i. C_ν is the carbon content of the plant functional type, defined by eqn. 22.

$$C_\nu = L + R + W \tag{22}$$

L, R and W are the different components of the vegetation carbon content, divided into (L)eaf carbon, (R)oot carbon and (S)tem carbon. The local litterfall rate, Λ_l, is given by:

$$\Lambda_l = \gamma_l L + \gamma_r R + \gamma_w W \tag{23}$$

γ_l,γ_r, and γ_w are the turnover rates of the different carbon pools. If we approximate eqn. 23 by

$$\Lambda_l \sim \frac{\gamma_l + \gamma_r + \gamma_w}{3}(L + R + W) \tag{24}$$

Then comparing eqns. 24 and 22 we can see that we are in effect approximating Λ_l as $\Lambda_l \propto C_\nu$. This assumption is also made by Huntingford *et al.* (2000). However

Huntingford *et al.* (2000) do not claim that their model is TRIFFID. The TRIFFID equations can now be simplified to the one species case, expressed in terms of ν and C_ν. This form of TRIFFID is given in eqns. 25 and 26.

$$\frac{dC_\nu}{dt} = (1-\lambda')\Pi - \alpha C_\nu \tag{25}$$

$$\frac{d\nu}{dt} = \frac{\lambda'\,\Pi\nu}{C_\nu}(1-\nu)\ - \gamma\nu \tag{26}$$

NPP is initially held constant. The λ function is originally a function of balanced leaf area index (balanced leaf area index is the LAI value before phenological constraints are applied), but leaf area index is approximately proportional to C_ν (Huntingford *et al.* (2000)) and so we can approximate the original λ function by a function of vegetation carbon content, given in eqn. 27.

$$\lambda' = \begin{cases} 1 & \text{for } C_\nu > C_{max} \\ \frac{C_\nu - C_{min}}{C_{max} - C_{min}} & \text{for } C_{min} < C_\nu \leq C_{max} \\ 0 & \text{for } C_\nu \leq C_{min} \end{cases} \tag{27}$$

C_{min} and C_{max} are the carbon densities corresponding to the maximum and minimum LAI values. The values of constants in eqns. 25, 26, and 27 are given in table 2. The value of α is chosen such that the behaviour of the simplified form of TRIFFID matches as closely as possible that of the full complexity TRIFFID.

	BL	NL	C3	C4	SH
γ $(year^{-1})$	0.004	0.004	0.100	0.100	0.030
C_{max} $(kgC\ m^{-2})$	26.0	27.1	0.3	0.5	2.0
C_{min} $(kgC\ m^{-2})$	4.3	4.7	0.1	0.1	0.2

Table 2: *Values of constants, for each PFT. α must be chosen so the behaviour of the simplified model matches that of the full complexity model. This method was used in Huntingford* et al. *(2000). The γ values presented here are reproduced from Cox (2001). C_{max}, and C_{min} values are equivalent to minimum and maximum leaf area index values presented in Cox (2001).*

5 Validation

In order to test the ability of the simplified model to successfully capture the behaviour of the TRIFFID model, the simplified model is forced with a dataset of NPP, from a control run of MOSES2. The vegetation fractional coverage predicted by the simplified model is then compared to the fractional coverages predicted in the full TRIFFID model. Figure 4 compares the simplified model predicted fractional coverage of C4 grass, for an Australian grid box. Grass was chosen because it exhibits high variability, and therefore provides the most stringent test of the simplified model. Other tests were performed for land surfaces dominated by other PFTs. The shrub and tree PFTs do not exhibit as great variability as the grass PFTs, and because the simplified model requires that a suitable choice of α be selected these other tests are not particularly demanding. Therefore reproducing the high variability of grass PFT structure is the

best test of the simplified model.

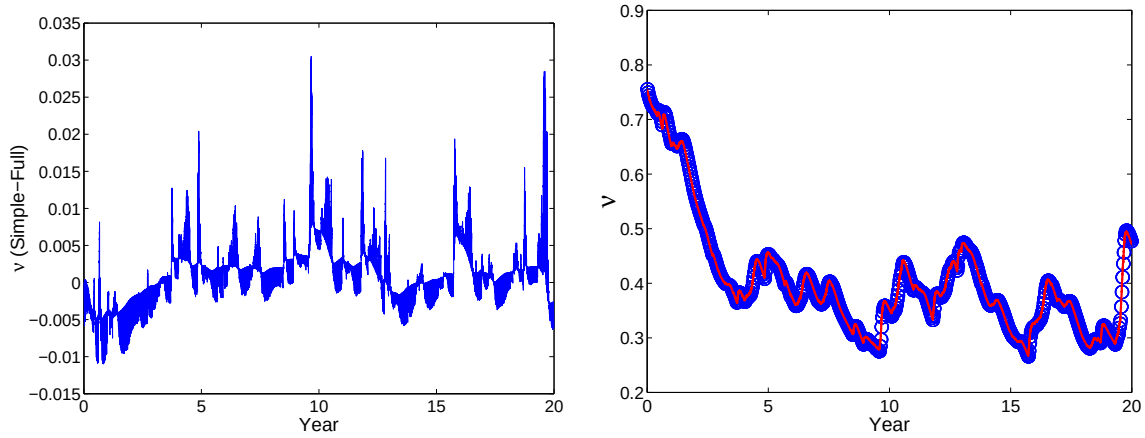

(a) (b)

Figure 4: *Comparison of fractional coverages from the full complexity TRIFFID DGVM, and from the simplified model, forced with identical net primary productivity. This is for an Australian grid box. a) shows the difference between simple model fractional coverage and the full complexity TRIFFID. b) shows the fractional coverage from the full complexity model and the simplified model. The full complexity TRIFFID fractional coverage is plotted with blue circles, and the simplified model predicted fractional coverage is plotted with a solid red line. For the simple model, a choice of* $\alpha = 8.0\times 10^{-9}$ *year*$^{-1}$ *gave the best fit to the behaviour of the full complexity model. This value was derived through a method of trial and error.*

Figure 4 shows that the simplified model is fully capable of reproducing the behaviour of the TRIFFID model. It suggests that results from analysis of the simplified model are directly applicable to the full TRIFFID model. We will therefore analyse the properties of this simplified model

6 Steady state solutions of the simplified model

Figure 5 simulates the re-growth from a small seeded amount (1×10^{-4} % fractional coverage, and 1×10^{-6} kg C m^{-2} s^{-1}) of the broadleaf and needleleaf tree. As can be seen in fig. 5, the re-growth of the fractional coverage is much slower in coming to equilibrium than the carbon density. The difference in behaviour between the two tree PFTs is due to the different values of C_{max} and C_{min} (see table 2). The 's' shaped pattern of fractional coverage recovery is characteristic of the logistic equation (which has the general form : $\frac{dX}{dt} \propto X(1-X)$). The logistic equation is characterised by an initially slow growth rate, when the population size (or fractional coverage) is small. Next the population undergoes rapid expansion, until the effects of over-crowding slow the population expansion rate down, and the curve reaches a steady state.

The steady state solutions of the simplified model equations are found by setting the time derivatives to zero, and by solving the resulting equations. Doing this leads

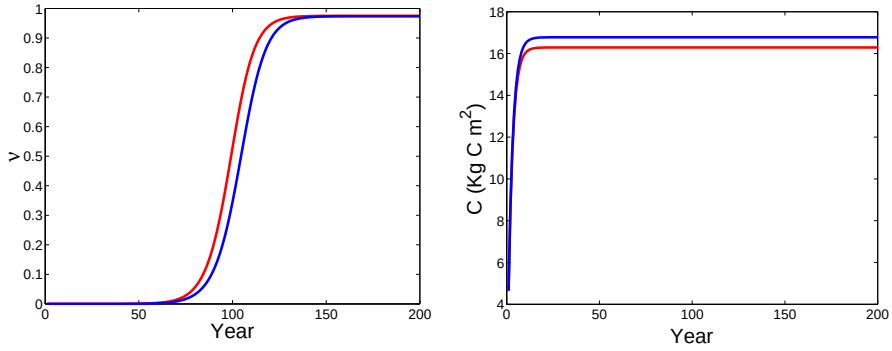

(a) (b)

Figure 5: *Simulation of broadleaf and needleleaf re-growth from bare soil using the simplified TRIFFID model. a) Fractional coverage. b) Carbon density. These figures show the re-growth from a small initial population of the two tree PFTs. Both PFTs have been individually simulated, and the two runs are over-laid for comparison. Broadleaf tree is shown as the red line, whilst needleleaf tree is shown as the blue line. In simulating the tree's re-growth the values for model constraints were taken form table 2,* α *was set to 0.128 year*$^{-1}$*. NPP =* 1.57×10^{-7} *kg C m*$^{-2}$ *s*$^{-1}$*. Values of* α *and NPP were chosen so that the re-growth of trees took a realistic time (similar to that observed in studies presented in Hughes (2003)). The merit of these plots is not in the prediction of the re-growth timescales, but in illustrating the intrinsic differences between the different tree PFTs, and the general pattern of re-growth common to all PFT.*

to eqns. 28 and 29.

$$\nu_{ss} = 1 - (\frac{\gamma}{\alpha})(\frac{1-\lambda'}{\lambda'}) \tag{28}$$

$$C_{ss} = \frac{(1-\lambda')\Pi}{\alpha} \tag{29}$$

When λ' takes the form of expression 27, the steady state solution is :

$$\nu_{ss} = 1 - \frac{\gamma}{\alpha}(\frac{(C_{max} - C_{min} + \frac{\Pi}{\alpha})}{(\frac{\Pi}{\alpha} - C_{min})} - 1) \tag{30}$$

$$C_{ss} = \frac{\Pi}{\alpha}(1 - \frac{(\frac{\Pi}{\alpha} - C_{min})}{(C_{max} - C_{min} + \frac{\Pi}{\alpha})}) \tag{31}$$

When the steady state fractional coverage is plotted as a function of net primary productivity, fig. 6, we see that below a cut off value of NPP, which will be referred to as $\Pi(*)$, the steady state fractional coverage is zero. For NPP $\leq \Pi(*)$ the growth rate is less than the harvesting rate and the population cannot expand. For NPP values greater than $\Pi(*)$ the fractional coverage increases non-linearly as a function of NPP. Initially the rate of change of ν_{ss} with respect to NPP is relatively large, and ν_{ss} is sensitive to small increases in NPP. For larger values of NPP the rate of change of ν_{ss} with respect to NPP is relatively small, and ν_{ss} is insensitive to increases in NPP. The absolute values of NPP vary for different PFTs, however, as NPP approaches some

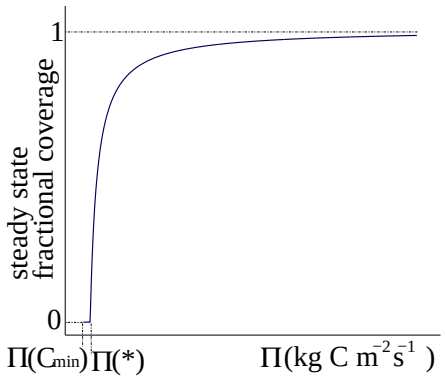

Figure 6: *The generic steady state response of vegetation fractional coverage to NPP (*Π*). The x-axis shows NPP. The y-axis shows steady state fractional coverage.*

value, Π', such that ν_{ss} approaches 1, the vegetation structure becomes increasingly insensitive to further increases in NPP, because of the substantial over-crowding effects at this point on the curve. C_{ss} has a similar non-linear response, without the threshold level value of $\Pi(*)$.

7 Initial growth rates

The intrinsic growth rate (r_i) is the rate of population expansion in a completely unrestricting environment (i.e. without the effects of overcrowding). Lotka-Volterra type equations have one main timescale of variability (τ), which is the inverse of the intrinsic growth rate, $\tau = 1/r_i$. In the simplified TRIFFID model the intrinsic growth rate is given by:

$$r_i = \frac{\lambda' \Pi}{C} - \gamma \tag{32}$$

Equation 32 shows that the intrinsic growth rate is a linear function of net primary productivity. It also shows that the response time of the TRIFFID model is inversely proportional to carbon density. As NPP decreases towards $\Pi(*)$, τ increases towards infinity.

In the section 6 it was stated that below NPP= $\Pi(*)$ the steady state fractional coverage is zero. The interpretation of this is that at $\Pi(*)$ the growth rate (r_i) =0. Therefore from eqns. 31 and 32 it can been derived that:

$$\Pi(*) = \alpha[\frac{\alpha C_{min}(C_{max} - C_{min})}{1 - \gamma(C_{max} - C_{min})} + C_{min}][1 - \frac{\alpha C_{min}}{1 - \gamma(C_{max} - C_{min})}]^{-1} \tag{33}$$

In this report several different timescales are referred to. It important to define the relationships between these different timescales. The generic logistic curve has the form $\frac{d\nu}{dt} = r_i \nu(1 - \nu)$. r_i is the intrinsic growth rate. ν is the population size (in non-dimensional units). The maximum size of ν is assumed to be 1. When ν is small, $\frac{d\nu}{dt}\frac{1}{\nu} = r_i$. Therefore the intrinsic growth rate is equivalent to the initial growth rate.

The logistic equation has solutions of the form:

$$\nu(t) = \frac{1}{1+be^{-r_i t}} \tag{34}$$

This form of the logistic equation can then be used to relate the intrinsic growth rate to the re-growth timescale. The time taken to re-grow is assumed to be the time take to re-grow from ν_{init} to ν_{final}, *i.e.* the re-growth timescale is assumed to be the time taken to re-grow from a very small fractional coverage to some value close to the maximum possible fractional coverage. Figure 5(a) shows that as fractional coverage approaches the maximum possible value the re-growth slows down, and so it is necessary to consider re-growth to some percentage of the maximum possible population as having re-grown. Constraining eqn. 34 to the initial condition $\nu(0)$=ν_{init} we have:

$$\nu(t) = \frac{1}{1+(\nu_{init}^{-1}-1)e^{-r_i t}} \tag{35}$$

and then the time taken to reach ν_{final} is given by:

$$re-growth\ \ time = \frac{1}{r_i} ln[(\nu_{final}^{-1}-1)(\nu_{init}^{-1}-1)^{-1}]^{-1} \tag{36}$$

This shows that the re-growth time, and indeed the time taken to change between any two values of ν is determined by the intrinsic growth rate and the two values of ν. Therefore the recovery from a 4% reduction in fractional coverage, the re-growth from near-bare soil conditions, and the initial re-growth rate are all governed by the same parameter, r.

8 Maximum rate of expansion and stability analysis

Equation 26 can be rearranged as :

$$\frac{d\nu}{dt} = (\frac{\lambda\Pi}{C}-\gamma)\nu - \frac{\lambda\Pi}{C}\nu^2 \tag{37}$$

A plot of $\frac{d\nu}{dt}$ against ν takes the form of a parabola, fig. 7. The zeros of $\frac{d\nu}{dt}$ are $\nu = 0$ and $\nu = 1-\frac{\gamma C}{\lambda\Pi}$. The maximum value of $\frac{d\nu}{dt}$ is at $\nu = (1-\frac{\gamma C}{\lambda\Pi})/2$, and the maximum rate of expansion is given by :

$$\frac{d\nu}{dt}|_{max} = \frac{\gamma^2 C}{2\Pi\lambda} \tag{38}$$

Figure 7 also demonstrates the stability of the model, for positive fractional coverages. At fractional coverages greater than $\nu = 1-\frac{\gamma C}{\lambda\Pi}$ the change in fractional coverage

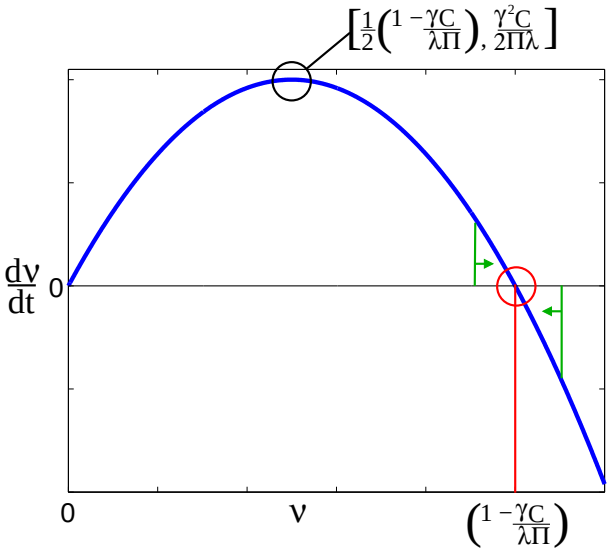

Figure 7: *Parabola properties of the simplified TRIFFID model. This figure shows the stability properties of the fractional coverage, ν. Marked on this figure is the maximum rate of expansion, and the maximum fractional coverage. The green lines and arrows indicate that if displaced from the equilibrium point marked with a red circle the system will return to the equilibrium point. This is therefore a stable equilibrium.*

is negative, and the fractional coverage decreases. For fractional coverages less than $\nu = 1 - \frac{\gamma C}{\lambda \Pi}$ the change in fractional coverage is positive, so perturbations away from the equilibrium point decay, and the model is stable.

In the discrete form of the logistic equation, equations can exhibit chaotic behaviour (May (1976)). However this is numerical chaotic behaviour of the discrete logistic equation, and it means that there is a limit to the size of possible timesteps. This effect is important when the timestep size is equal to 1 year, but is eliminated when a timestep of 10 days is used (tests were performed for grass plant functional types, as with the fastest response time they are most prone to chaotic effects). This emphasises the need to use relatively small timesteps.

9 Internal variability

The values of NPP in the full TRIFFID model are not constant, and are associated with the variability of meteorological surface conditions. The effect of forcing the simplified TRIFFID model with stochastic net primary production is investigated in this section.

There is considerable intra-annual variability of simulated grass structure in TRIFFID. The simple model is ideal for investigating the source of this variability. When the simplified model is run with a constant value of NPP, the fractional coverage does not vary between timesteps. A randomly generated data set of white noise NPP values are used to force the simple model. When this is done, as is seen in fig. 8, the vegetation structure also exhibits stochastic-like variability. The random NPP values mimic the natural variability of environmental conditions. When forced by stochastic NPP the model still exhibits convergence behaviour. This means that the model is still

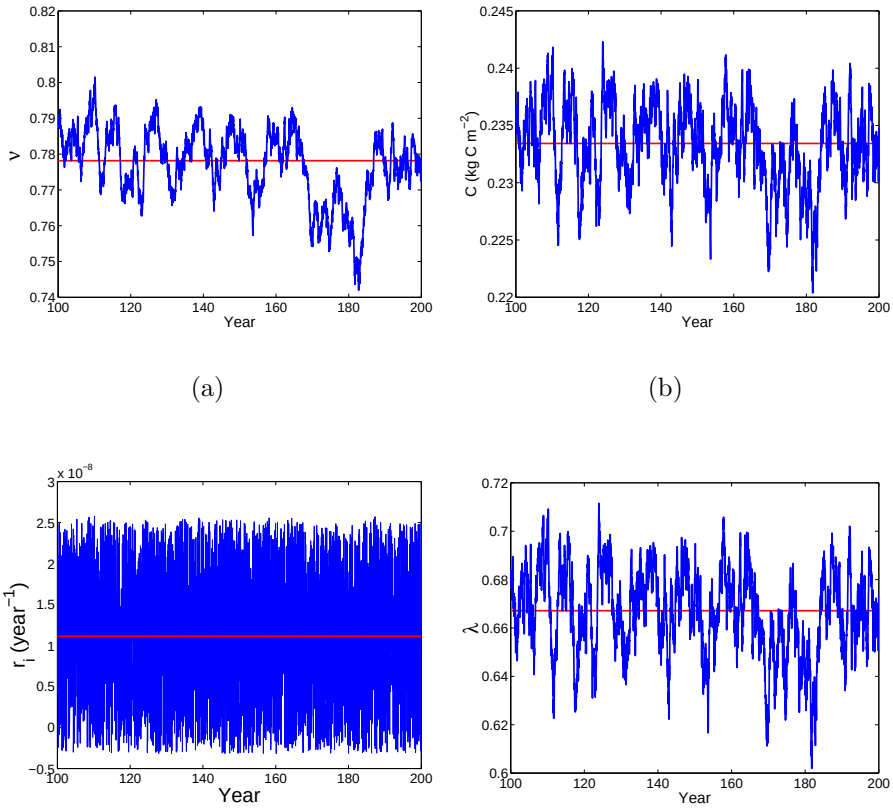

Figure 8: *The effect of forcing the simplified model with stochastic NPP, for C3 type grass. a) Fractional coverage. b) Carbon density. c) Intrinsic growth rate. d) λ function. The red line shows the grass behaviour for constant NPP. The blue line shows the behaviour of C3 type grass with a stochastic NPP term.* $\alpha = 7.13\times10^{-9}\ s^{-1}$. $\overline{NPP} = 5\times10^{-9}\ kg\ C\ m^2\ s^{-1}$. *The amplitude of noise added to* $\overline{NPP} = 5\times10^{-9}\ kg\ C\ m^2\ s^{-1}$. *Values of* α *and* $\overline{NPP}$ *were chosen such that the re-growth from bare soil was realistically simulated. The amplitude of noise added was chosen to maximize the observed variability in vegetation structure.*

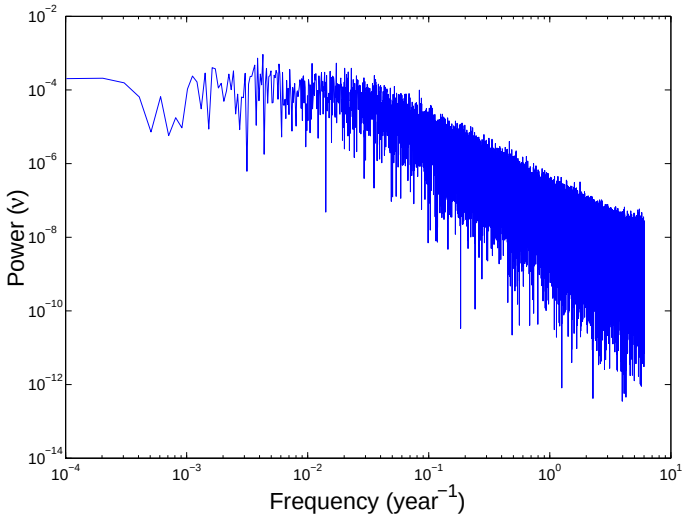

(a)

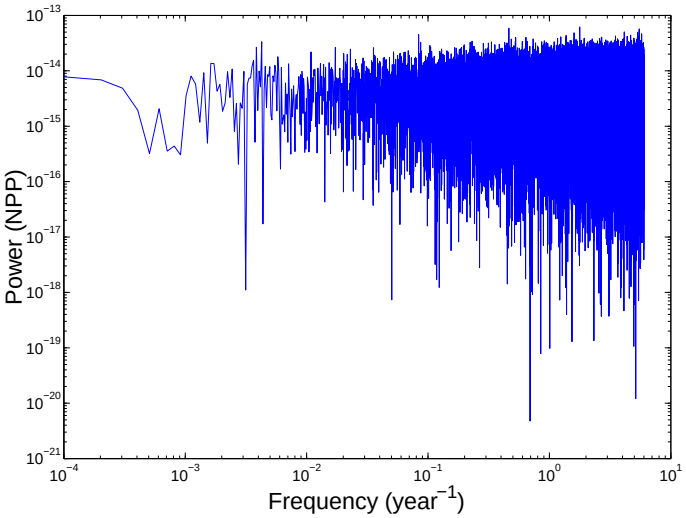

(b)

Figure 9: *a) the spectral profile of vegetation fractional coverage fluctuations. b) the spectral response of the NPP data set used to force the simplified model. In both figures the y-axis shows the power at a given frequency, whilst the x-axis shows the frequency. The model was run with monthly timesteps, and the data set length was 10,000 years.* $\overline{NPP}$*=1.57*$\times 10^{-7}$ *kg C* m^2 s^{-1}*. The white noise amplitude is 1.25*$\times 10^{-7}$ *kg C* m^2 s^{-1}*.* α*=0.128* $year^{-1}$*. These values were chosen such that the re-growth from a small initial fractional coverage was realistically simulated. The amplitude of the white noise was chosen to maximize variability of fractional coverage.*

stable even when forced with random NPP datasets (which represents the variability of environment conditions in the full model). A system is generally considered stable if small differences in the initial conditions remain close together (Khalil (1996) p. 97).

In order to investigate the role of the intrinsic timescale in the observed variability of vegetation structure the spectral profile of the changes in fractional coverage was calculated, when the simplified model was forced with a white noise NPP data set. The simple model was run with broadleaf tree parameter values. Figure 9 shows the spectral profiles of both the NPP data and the corresponding fractional coverage changes. Figure 9 shows that when the simplified model is forced with white noise NPP it responds with red noise variability. This means that high frequency noise in the NPP data set is damped out. The frequency above which the variability is damped corresponds to the time taken to re-grow from near-bare soil conditions ($\sim$100 years). TRIFFID therefore acts as a climatic integrator below these timescales. This is also a general feature of individual trees (Woodward (1987)). The attenuation of timescales less than the characteristic response time was also shown by Lasaga and Berner (1998) to occur for the geological terrestrial carbon cycle. Henderson-Sellers (1993) state that this property of the global vegetation model is an important component of modelling global vegetation dynamically.

An additional feature discussed by Woodward (1987) is that trees tend to have an increased response to climate close to the characteristic timescale. This is equivalent to stating that the trees *resonate* at their characteristic timescale (for a mathematical definition of resonance see Thomson (1993)). The TRIFFID model does not explicitly include resonance (this can be seen in fig. 9), but may exhibit resonant behaviour when coupled to the ocean (through the atmosphere), as was the case in the conceptual model of Nevison *et al.* (1999). This would be hard to detect in the Hadley Centre model, and there is no evidence for vegetation-oceanic resonance at present. There is also no clear resonant peak in the suite of models discussed by Mitchell and Karoly (2001), which includes the HadCM3 GCM.

10 Validation of re-growth times

Validation of the behaviour of the dynamical vegetation model is problematic, because of the length of observations required (Woodward and Beerling (1997)). One source of possible validation is the recovery of vegetation after the 1908 near-impact of an meteorite. On June the 30th, 1908, a large meteorite exploded 5-10km above Tunguska in western Siberia (60 N , 101 E). The blast is thought to have started forest fires, and photographic evidence shows that a large area ($\sim$ 2,000 km^2) of trees was uprooted (Vasilyev (1998)). At this latitude a HadSM3 grid box covers an area of approximately 55,000 km^2. The Tunguska perturbation therefore corresponds to a near-instantaneous reduction of fractional coverage of 4 %.

Given the site's obvious cosmological value the site has been repeatedly visited, however scientific literature on the Tunguska meteorite is usually cosmological, and often in Russian language (see Jones (2002); Svetsov (2002)). Detailed information on the fractional coverage of the disturbance is therefore unavailable (T.P. Jones *pers. com.* 2003). Photographic evidence suggests, however, that the disturbance region had been re-colonised by 1990, which is taken here to show a recovery time of 80 years.

HadSM3 predicts dense needleleaf forest at the Tunguska grid box in the pre-agricultural simulation, which approximates the observed swampy forest at the Tunguska site. The Tunguska grid box is then represented in the simple model as entirely needleleaf tree, and the Tunguska meteorite event as an instantaneous reduction if needleaf fractional coverage by 4 %. Figure 10 shows the predicted response of the grid box fractional coverage of needleleaf trees to this perturbation.

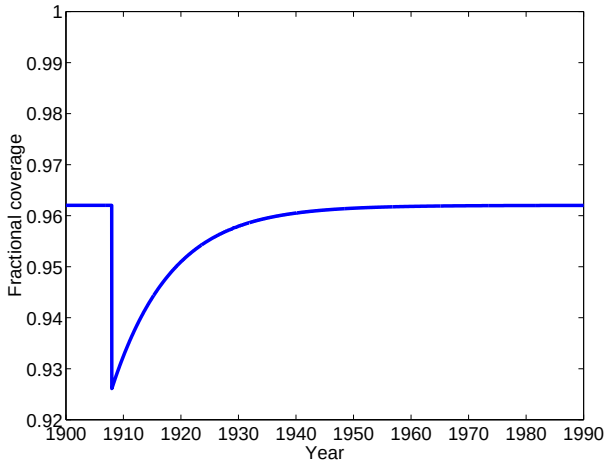

Figure 10: *Simulated re-growth of needleleaf tree PFT from the effect of the Tunguska meteorite in 1908. Values of NPP = 1.1×10^{-7} kg C m^{-2} s^{-1}, α = 4.12×10^{-9} s^{-1} were used. These values were chosen as they produced a re-growth from bare soil time of 125 years for needleleaf tree.*

Figure 10 shows that the simplified model predicts a full re-growth of needleleaf tree coverage by the mid 1990's, and is in agreement with what is know of the Tunguska site. Figure 10 also illustrates an important feature of the simplified model (and hence the full model). If instead of modelling the entire grid box the simplified model had been used to simulate vegetation re-growth only in the region of disturbed trees, the re-growth would have followed the same pattern as is shown in fig. 5, and the re-growth would have taken much longer (125 years). This demonstrates a clear scale dependence in the TRIFFID model.

11 Conclusions

The aim of this study was to investigate the properties of the population model relevant to properties of the vegetation-climate system in the TRIFFID model, and in order to perform this a simplified version of TRIFFID was developed and analysed.

The approximations made in developing the simplified form of the TRIFFID equations appear to have minimal effect. The assumption of a single plant functional type has been shown to be reasonable for the majority of global vegetation, but obviously constrains the model to simulating the dominant plant functional type. The assumption of constant litterfall and disturbance rates means that appropriate constants must be chosen to match the vegetation dynamics of the full model, but once this is done the simplified model captures the variability of the model. The main limitation is that the photosynthesis model was not coded explicitly into the model. The photosynthesis model, however, simply acts to translate climatic conditions into net primary

productivity, and has been discussed elsewhere (see Cox (2001)). The net primary productivity has therefore been either specified, or set to a constant value with stochastic variability. Huntingford *et al.* (2000) present a simplified terrestrial carbon cycle which does simulate photosynthesis rates, and including this feature into the simplified model would only increase the model complexity without adding anything new.

Analysis of the TRIFFID equations suggests that the TRIFFID model parameters allow for stable coexistence. The fact that competing vegetation types are seen to be approximately mutually exclusive suggests that the plant functional types exist in a largely exclusive climatological niche. Analysis of TRIFFID equations suggests that the simulated transition between plant functional types is smooth, rather than discrete (see Svirezhev (2000)). From the simplified TRIFFID model it can be seen that the fractional coverage is the slowest component of the TRIFFID system. Figure 5 shows that for tree PFTs, the carbon density has reached a steady state after 10 years, whilst fractional coverage takes 125 years to reach a steady state.

Data sets of net primary production and the vegetation structure were calculated in the full complexity surface energy scheme. Grid boxes where the dominant vegetation type was C4 type grass were chosen. Grass shows the largest variability in structure, and is therefore the most stringent test for the simplified model. The generated datasets of NPP were used to drive the simplified model, and the predicted vegetation structure was compared to that simulated by the full complexity model. Given the reduction in sophistication associated with assuming a single plant functional type, and constant litterfall parameters, the simplified model captures the behaviour of the full complexity model surprisingly well.

Equations governing the steady state of the vegetation structure have been derived. They show the existence of a threshold value of NPP, below which vegetation coverage is zero. These equations also show that the steady state vegetation structure is insensitive to further increases in NPP as NPP becomes large. This insensitivity is due to the assumption that vegetation fractional coverage can be modelled using a logistic curve (see fig. 5(a)).

The initial growth rate and the maximum growth rate have been diagnosed. Both rates are dependent on the NPP. The initial growth rate is equivalent to the intrinsic growth rate, and is the reciprocal of the vegetation structure response time. The fractional coverage response time is the most important timescale (and hence the general response time) as it is the slowest response time of the TRIFFID model. This response time acts as a climate integrator, smoothing the effects of climate on the fractional coverage, and filtering out climate variability at frequencies above the response time. The response time also acts to provide a vegetation memory, perturbations to the vegetation structure decay at the response time of the vegetation. Further work is required to investigate how this affects the atmospheric variability. The results described here suggest that vegetation structure will change a white noise spectrum to red noise.

The population model exhibits convergence, even when forced with stochastic NPP, which means that the model is stable. It can therefore be concluded that the model is not a source of chaos. The simulated variability in grass structure (*e.g.* fig. 4) is therefore driven by variability in the meteorological conditions (potentially with feedbacks from the vegetation), rather than internal model variability. However the response time which is an internal feature of TRIFFID determines how much the stochastic meteorological signal is damped, and hence provides some internal control over the

observed variability.

The timescales of response have been tested against observations of a well dated perturbation, on the spatial scale of an atmospheric grid box. The timescale of response predicted by the model is similar to that observed. The discussion of the response to a small perturbation also shows that the behaviour of the dynamic vegetation is scale dependent. It is hoped that the results presented in this study will be useful for interpretation of results from future GCM experiments.

References

Case, T. (2000). *An illustrated guide to theoretical ecology.* Oxford University Press, Oxford, UK.

Cox, P. (2001). Description on the TRIFFID Dynamic Global Vegetation Model. Technical Report 24, Hadley Centre, Met Office.

Cox, P., Huntingford, C., and Harding, R. (1998). A canopy conductance and photosynthesis model for use in a GCM land surface scheme. *Journal of Hydrology*, **213**, 79–94.

Gotelli, N. (1998). *A primer of Ecology.* Sinauer Associates, Inc. Publishers, Sunderland, Massachusetts, 2nd edition. pp. 200.

Henderson-Sellers, A. (1993). Continental vegetation as a dynamic component of a global climate model: a preliminary assessment. *Clim. Change*, **23**, 337–377.

Hughes, J. (2003). *The Dynamic Response of the Global Atmosphere-Vegetation coupled system.* Ph.D. thesis, Department of Meteorology, University of Reading.

Huntingford, C., Cox, P., and Lenton, T. (2000). Contrasting responses of a simple ecosystem model to global change. *Ecological Modelling*, **134**, 41–58.

Jones, T. (2002). Reply "Extraterrestrial impacts and wildfires". *Palaeogeogr. Palaeoclimatol. Palaeoecol.*, **185**(3-4), 407–408.

Khalil, H. (1996). *Nonlinear Systems.* Prentice Hall, Upper Saddle River, 2nd edition. pp. 557.

Lasaga, A. and Berner, R. (1998). Fundemental aspects of quantitative models for geochemical cycles. *Chemical Geology*, **145**, 161–175.

May, R. (1976). Simple mathematical models with very complicated dynamics. *Nature*, **261**(5560), 459–467.

Mitchell, J. and Karoly, D. (2001). *Detection of Climate Change and Attribution of Causes In:Climate Change 2001: The Scientific Basis.* Cambridge University Press, Cambridge.

Nevison, C., Gupta, V., and Klinger, L. (1999). Self-sustained temperature oscillations on daisyworld. *Tellus*, **51B**, 806–814.

Svetsov, V. (2002). Comment on "extraterrestrial impacts and wildfires". *Palaeogeogr. Palaeoclimatol. Palaeoecol.*, **185**(3-4), 403–405.

Svirezhev, Y. (2000). Lotka-volterra models and the global vegetation pattern. *Ecological Modelling*, **135**, 135–146.

Thomson, W. (1993). *Theory of Vibration with Applications.* Nelson Thornes Ltd, Cheltenham, UK., 5th edition. pp. 560.

Vasilyev, N. (1998). The tunguska meteorite problem today. *Planetary and Space Science*, **46**(2-3), 129–150.

Woodward, F. (1987). *Climate and Plant Distribution.* Cambridge University Press, cambridge, UK. pp. 190.

Woodward, F. and Beerling, D. (1997). The dynamics of vegetation change: health warnings for equilibrium 'dodo' models. *Global Ecology and Biogeography Letters*, **6**, 413–418.